Atmos. Chem. Phys. Discuss., 9, 13775–13799, 2009
www.atmos-chem-phys-discuss.net/9/13775/2009/

Atmospheric Chemistry and Physics Discussions

This discussion paper is/has been under review for the journal *Atmospheric Chemistry and Physics (ACP)*. Please refer to the corresponding final paper in *ACP* if available.

Slower CCN growth kinetics of anthropogenic aerosol compared to biogenic aerosol observed at a rural site

N. C. Shantz[1,*], **R. Y.-W. Chang**[1], **J. G. Slowik**[1], **J. P. D. Abbatt**[1], **and W. R. Leaitch**[2]

[1]Department of Chemistry, University of Toronto, Toronto, Ontario, Canada
[2]Climate Research Division, Science and Technology Branch, Environment Canada, Toronto, Ontario, Canada
[*]now at: Cloud Physics and Severe Weather Research Section, Science and Technology Branch, Environment Canada, Toronto, Ontario, Canada

Received: 1 June 2009 – Accepted: 8 June 2009 – Published: 23 June 2009

Correspondence to: N. C. Shantz (nicole.shantz@ec.gc.ca)

Published by Copernicus Publications on behalf of the European Geosciences Union.

Abstract

Growth rates of water droplets were measured with a static diffusion cloud condensation chamber in May–June 2007 at a rural field site in Southern Ontario, Canada, 70 km north of Toronto. Observations were made during periods when the winds were from the south and the site was impacted by anthropogenic air from the US and Southern Ontario as well as during a 5-day period of northerly wind flow when the aerosol was dominated by biogenic sources. The growth of droplets on anthropogenic size-selected particles centred at 0.1 μm diameter and composed of approximately 40% organic and 60% ammonium sulphate (AS) by mass, was delayed on the order of 1 second compared to a pure AS aerosol. Simulations of the growth rate indicate that a lowering of the water mass accommodation coefficient from α_c=1 to an average of α_c=0.044 is needed (assuming an insoluble organic with hygroscopicity parameter, κ_{org}, of zero). In contrast, the growth rate of the aerosol of biogenic character, consisting of >80% organic, was similar to that of pure AS. Simulations of the predominantly biogenic aerosol show agreement between the observations and simulations when κ_{org}=0.05–0.2 and α_c=1. Inhibition of water uptake by the anthropogenic organic applied to an adiabatic cloud parcel model in the form of a constant low α_c increases the number of droplets in a cloud compared to pure AS. If the α_c is assumed to increase with increasing liquid water on the droplets, then the number of droplets decreases which could diminish the indirect effect. The slightly lower κ_{org} in the biogenic case decreases the number of droplets in a cloud compared to pure AS.

1 Introduction

Aerosol particles affect the atmospheric radiation budget directly by scattering or absorbing radiation and indirectly by acting as cloud condensation nuclei (CCN). If the amount of cloud liquid water does not change with changes in CCN, then an increase in the number of droplets leads to a decrease in the size of the droplets with increas-

ACPD

9, 13775–13799, 2009

ing CCN, thus influencing the radiative properties and lifetimes of clouds. The extent of the cloud indirect effect of aerosol particles is highly uncertain (IPCC, 2007), and part of this uncertainty is understanding how the organic components contribute to the formation of cloud droplets. Carbonaceous material represents a significant fraction of atmospheric fine particle composition (Zhang et al., 2007). Mixtures of organic and inorganic components are complex and water uptake is difficult to characterize. The literature contains many examples of laboratory studies of the CCN behaviour of organic aerosol particles (e.g. Abbatt et al., 2005; Cruz and Pandis, 1997; Shantz et al., 2003; Shulman et al., 1996) but currently, the focus is moving away from studying organics alone in the laboratory and moving towards studying the CCN character of ambient aerosols from different sources (i.e. mixtures that may contain organics) (e.g. Chang et al., 2007; Ruehl et al., 2008; Shantz et al., 2008; Stroud et al., 2007).

Two significant sources of organic aerosols are the oxidation products of biogenic emissions (e.g. monoterpenes) and anthropogenic emissions (primary as well as oxidation products of anthropogenic volatile organic compounds, or VOCs). Organic biogenic aerosols have been found to be reasonably CCN active in smog chamber studies (e.g. Duplissy et al., 2008; Hartz et al., 2005; Prenni et al., 2007; VanReken et al., 2005). Duplissy et al. (2008) found the aerosol formed from α-pinene oxidation became more CCN active over time when exposed to sunlight. VanReken et al. (2005) found the CCN activity to decrease as more oxidation products condensed on the aerosol in a dark experiment. Field observations of biogenic aerosols suggest that this organic contributes to the CCN activity (Leaitch et al., 1999; Shantz et al., 2008). In contrast, several field studies focussed on anthropogenic emissions suggest that CCN closure is easily achieved if an insoluble organic is assumed, showing that the sulphate present in the aerosol dominated the CCN activity (Broekhuizen et al., 2006; Medina et al., 2007; Stroud et al., 2007). A number of studies suggest that the contribution of the organic components to the CCN activity increases when more of the organic component is assumed to be soluble (e.g. Chang et al., 2007; Ming and Russell, 2004).

The recent introduction of a single hygroscopicity parameter, κ, reduces the large

ACPD
9, 13775–13799, 2009

number of physical and chemical parameters needed to describe the water uptake by growing droplets to one value (Petters and Kreidenweis, 2007). For aerosols consisting of multiple components, the value of κ_{tot} is given by a simple mixing rule: $\kappa_{tot} = \sum \varepsilon_i \kappa_i$, where ε_i is the volume fraction and i is the index representing the individual species (Petters and Kreidenweis, 2007). This parameter has been determined for organic particles resulting from the oxidation of biogenic VOCs in smog chamber studies as 0.1 (Duplissy et al., 2008; Prenni et al., 2007) and 0.15 (Engelhart et al., 2008) and 0.02–0.05 in a biogenic field study (Shantz et al., 2008).

Chuang et al. (1997) showed that neglecting kinetic limitations on the water uptake of cloud droplets can lead to overestimations in cloud radiative forcing calculations and thus kinetics should be considered. The water vapour mass accommodation coefficient, α_c, can have a strong effect on the condensation rate of water and remains an outstanding uncertainty in quantifying the indirect effect of aerosols on climate forcing. Literature values of α_c span 2 orders of magnitude, from 0.01 to 1 (e.g. Davidovits et al., 2004; Laaksonen et al., 2005; Marek and Straub, 2001; Mozurkewich, 1986, and the references therein) and have been estimated to be as low as 10^{-5} for organic films on cloud droplet surfaces (Chuang, 2003). Ruehl et al. (2008) found that approximately 60% of the ambient CCN of urban, polluted regional and continental origins grew into cloud droplets at a similar rate as ammonium sulphate (AS). They observed a number of cases that had a lower α_c compared to AS at various sites.

In this paper, observations from a field study at Egbert, Ontario, Canada during the late spring of 2007 are used to contrast the CCN cloud droplet water uptake by aerosol particles containing organics from anthropogenic vs. biogenic sources. The CCN water uptake growth kinetics were studied using a cloud droplet growth model that utilizes κ to determine the hygroscopicity of the organic aerosol (Shantz et al., 2008). The rate of growth of aerosol particles containing anthropogenic organic components is found to be reduced.

ACPD
9, 13775–13799, 2009

2 Experiment

The Egbert 2007 field campaign took place May-June 2007 at a rural field site in Southern Ontario, Canada, 70 km north of Toronto (44.23 N, 79.78 W, see Fig. 1). Previous studies of the atmospheric aerosol at this site are discussed by Chang et al. (2007) and Rupakheti et al. (2005).

2.1 Instrumentation

Much of the instrumentation used during the Egbert 2007 field campaign is described by Slowik et al. (2009), Vlasenko et al. (2009) and Chan et al. (2009). The focus of this work is on data from a static thermal diffusion chamber (University of Wyoming Model 100 CCN counter) used to study the initial growth rates of cloud droplets at a constant supersaturation (Shantz et al., 2003, 2008). The experimentally determined supersaturation used in this work is S=0.35±0.05%, found using nearly monodisperse ammonium sulphate particles as discussed in Shantz et al. (2003, 2008). The polydisperse ambient aerosol was sampled directly into the CCN counter and a TSI 3022 Condensation Particle Counter (CPC) through a 3/8″OD stainless steel tube approximately 3 m in length with an intake point approximately 1 m above the roof of the building. In order to reduce the effect of dry particle size on the droplet growth rates, ambient aerosol particles were also size-selected with a TSI 3081 Long Differential Mobility Analyzer (DMA) during periods with measurable particle number concentrations. After size selection, the nearly monodisperse particle flow was split for measurement using the CPC and the CCN counter. Measured ambient growth rates from the CCN counter were compared to those of pure ammonium sulphate (AS) calibration aerosol at similar size and number concentration as the measured ambient aerosol. The AS calibration aerosol was nebulized and then size-selected with the DMA.

Ambient aerosol particle size distributions between 0.01 μm and 0.4 μm geometric diameter were determined with a Scanning Mobility Particle Sizer (SMPS) comprised of a TSI 3071 DMA and a TSI 3010 CPC (TSI Inc., St. Paul, MN, USA).

ACPD
9, 13775–13799, 2009

An Aerodyne time-of-flight (C-ToF) Aerosol Mass Spectrometer (AMS) (Aerodyne Research, Inc., Billerica, MA, USA) provides size-resolved, non-refractory chemical composition of submicron aerosol particles measured in the range of approximately 0.07–0.7 μm vacuum aerodynamic diameter (D_{va}), where for spherical particles $D_{va}=\rho_p D_{geo}$, where ρ_p is the particle density and D_{geo} is the geometric diameter. Detailed descriptions of the AMS design, operation, quantification methods and calibration procedures are given elsewhere (Canagaratna et al., 2007; Drewnick et al., 2005; Jayne et al., 2000; Jimenez et al., 2003; Liu et al., 2007). The mass concentrations have been corrected for an average collection efficiency of 0.6 determined for this study (Slowik et al., 2009).

3 Results and discussion

3.1 Time series overview

Figure 2 shows a time series of wind speed and direction (Fig. 2a, dates/times are in local time, LT, Eastern Daylight Savings Time, EDT) and mass concentrations from the AMS (Fig. 2b) (Slowik et al., 2009). Air reaching the site from the south is typically influenced by anthropogenic sources from the US and the highly populated Southern Ontario region (e.g. 7 June in Fig. 1a). During times of southerly winds (Fig. 2a, red shades), high mass concentrations of organic and sulphate were measured (e.g. 31 May–3 June and 7–9 June inclusive).

When winds were from the north (Fig. 2a, blue shades), the aerosol mass concentrations were usually lower (Fig. 2b). An exception to this was near the end of the study, 9–13 June, when north winds persisted (with few anthropogenic sources) and air reaching the site has travelled over a large fetch of mixed forests (e.g. 13 June in Fig. 1b). Figure 2b shows the organic mass concentration increased steadily over this time period. The gas-phase and aerosol signatures as well as regional modelling indicates that the origin of most of the organic aerosol during this period was from the

ACPD
9, 13775–13799, 2009

oxidation of biogenic precursors (Slowik et al., 2009).

3.2 CCN growth kinetics of monodisperse aerosol

Examples of droplet growth curves of size-selected ambient particles compared to AS particles at S=0.35% are shown in Figs. 3a and 4a. The CCN counter detector voltage (Fig. 3a) is proportional to the cross section of the growing cloud droplets. The data of Fig. 3 were collected during a period when the winds were from the southwest (Fig. 1a) and the aerosol had crossed over populated Southern Ontario and the Ohio valley. The AS calibration aerosol begins to accumulate water at approximately 2 s and grows through 8 s. After 8 s, the water droplets begin to fall from the detection region and the signal decreases. The initial growth of the ambient anthropogenic aerosol is delayed relative to the AS particles.

A droplet growth model that mimics the chamber supersaturation (Shantz et al., 2003, 2008) was used to investigate possible explanations for the delayed growth of the ambient aerosol. The model is initiated with nearly monodisperse particles with approximately 87% of the particles centred at 0.1 μm and 13% of the particles centred at 0.14 μm (the doubly charged particle mode that exit the DMA). Figure 3b shows the model results limited to 5 s as well as the observed growth rates for the AS and ambient aerosols from Fig. 3a. Only the first 5 s are shown as the model does not include the droplet gravitational settling at larger droplet sizes. The left and right axes are scaled according to the AS calibration results (Shantz et al., 2008). We assume that the water mass accommodation coefficient, α_c, for the AS case is unity. Figure 3c shows the AMS time-of-flight chemical composition measurements. All conversions from D_{va} to D_{geo} were performed assuming spherical particles and using the following material densities: ρ_{AS}=1.77 g cm^{-3} and ρ_{org}=1.3 g cm^{-3}. The mass fractions of the ambient particles were estimated from the data shown in Fig. 3c to be 62% for AS and 38% for the organic component at D_{va}=0.13–0.19 μm (corresponding to D_{geo}=0.08–0.12 μm with midpoint D_{geo}=0.1 μm). Initially, we assumed the surface tension of water, a mass

ACPD
9, 13775–13799, 2009

accommodation coefficient of α_c=1 (Davidovits et al., 2004; Laaksonen et al., 2005; Mozurkewich, 1986), a κ_{AS} of 0.61 (Petters and Kreidenweis, 2007) and a κ_{org} of 0 (i.e. the organic was assumed to not contribute to the initial water uptake). Although there was a slight delay in the ambient simulations compared to the AS simulations, it is not nearly as significant as the observed delay, suggesting that the organic compounds present in the ambient aerosol inhibited water uptake by these CCN.

There are 2 adjustable parameters for matching the simulations to the observed growth curves, κ_{org} and α_c. Since κ_{org}=0 is already overestimating the observed delay, increasing κ_{org} will not help achieve agreement between the observations and simulations. Instead, lower values of α_c (0.04–0.06) produce delays closer to that observed. This result may be consistent with Stroud et al. (2007) who found that α_c=0.07 was needed to achieve closure in a case study of a pollution episode. If α_c increases with the accumulation of water on the particles, then it may explain the rise in the ambient growth curve after 4 s. The effect of an increasing α_c with water uptake will be discussed further in Sect. 3.4.

This analysis was performed for the 6 anthropogenic monodisperse cases observed on 3 different days during the field campaign and the results are summarized in Table 1. The delays in the initial growth rates of the CCN droplets were estimated by comparing the ambient growth rate with the corresponding AS calibration growth rate at the same size and number concentration. The α_c ranges from 0.02 to 0.06 and the mean α_c is 0.044.

The size-selected aerosol sampled during the biogenic period is shown in Fig. 4a. Figure 4b shows this period was dominated by an organic aerosol. Growth of the 0.12 μm biogenic aerosol is not delayed relative to the AS aerosol even though the majority of the aerosol is organic (Fig. 4b). Although our previous field studies have indicated a CCN-active biogenic aerosol (Leaitch et al., 1999; Shantz et al., 2008), the comparable CCN activity between the organic-dominated aerosol and the pure AS aerosol observed at Egbert was unexpected.

For simulations of the ambient aerosols, we applied an approximate chemical com-

position of 12% AS (κ_{AS}=0.61) and 88% organic mass fractions (varying κ_{org}) based on the AMS mass distribution (Fig. 4b) and assumed that α_c=1. For the κ_{org}=0 case, there is more delay simulated (not shown) than was observed, suggesting that the organic component has an elevated value of κ_{org} and is contributing to the water uptake. The aerosol numbers are extremely low in this case and the estimation of κ_{org} from the comparison of the simulations and observations can only be constrained within a range of 0.05–0.2. This of course is based on an α_c of 1, but it is possible that the value of κ_{org} is higher than 0.2, in which case α_c must be significantly lower than 1.

The AMS data suggest that the anthropogenic aerosol was more oxygenated than the biogenic aerosol (Slowik et al., 2009); the latter aerosol perhaps consisted of fresh, small and soluble organic compounds that activate readily. The fact that the more oxygenated anthropogenic aerosol exhibits characteristics that suggest it slows down the rate of water uptake and that the less oxygenated biogenic aerosol takes up water readily is counter to the more common concepts of organic CCN activation (Kanakidou et al., 2005). We suggest that the more oxygenated anthropogenic organic components may have a higher average molecular weight and be less soluble, and that the water uptake suppression may be due to organic films arising from the HOA coating the aerosol; however, we are comparing organic compounds from different sources and the individual types of organics measured in both of these cases are unknown. Ruehl et al. (2008) observed at least 1 day of moderate to strong condensational droplet growth inhibition relative to AS at each of the urban, polluted regional and continental sites, consistent with the present observations.

3.3 CCN growth kinetics of polydisperse aerosol

We compare the anthropogenic and biogenic CCN abilities further using polydisperse data from different days at S=0.35%. Because we could not produce an AS calibration with the exact polydisperse ambient aerosol size distribution, we rely on the model described in Sect. 3.2 to study the effects of chemical composition on water uptake.

Figure 5a shows the droplet growth rates of the anthropogenic aerosol observed

ACPD
9, 13775–13799, 2009

from the CCN counter for 1 June. The error bars show the uncertainties that arise from errors in the calibrated supersaturation. The model size distribution assumption (based on the SMPS) was set up as shown in Fig. 5b. From the chemical mass distribution from the AMS (Fig. 5b), the growth rates were modelled assuming modes 1 and 2 consist of 50% AS and 50% organic and mode 3 consists of 60% AS and 40% organic (mass fractions) assuming κ_{org}=0. The best match with the observations is for the assumption of α_c=0.07 and α_c can be constrained within the supersaturation uncertainty to α_c=0.05–0.15, which are at the upper end of the result for the size-selected anthropogenic aerosol (Sect. 3.2).

Following the same procedure for a biogenic case (Fig. 6, with chemical composition assumptions that all 3 modes are 20% AS and 80% organic), we find that κ_{org}=0.2 (0.05 in the first few seconds of growth) and α_c=1 gives the best agreement between the model and the observed growth curves. The range κ_{org}=0.05-0.36 demonstrates the values within the supersaturation uncertainty. The biogenic organic must be contributing to the water uptake in this case as the levels of sulphate are low. These polydisperse experiments verify the findings from Sect. 3.2, which had higher uncertainties in the monodisperse biogenic case due to the much lower number concentrations.

3.4 Adiabatic cloud parcel model simulations

The results from the previous sections were used in an adiabatic cloud parcel model (Shantz et al., 2003) to consider the impact of the initial water uptake delay on the number concentrations of cloud droplets. Table 2 shows the number of activated droplets (N_d) above the maximum supersaturation in a cloud for updraft velocities of 20 cm s^{-1} and 100 cm s^{-1} and for aerosol number and chemical size distributions represented by the anthropogenic and biogenic observations. All size distributions are scaled to 1500 cm^{-3} total number concentration for simpler comparison.

The biogenic simulation included κ_{org}=0.2 and α_c=1 (Sect. 3.3) as well as a base case of pure AS. These assumptions lead to a lowering of the N_d to 0.80–0.89 of the N_d obtained for pure AS due to a lower κ_{org} (0.2) than κ_{AS} (0.61).

The anthropogenic simulation included κ_{org}=0 and α_c=0.044 (the average value found in Sect. 3.2) as well as a varying α_c that increased with increasing liquid water content (LWC) in each particle size bin. The base cases were run with the same chemical size distributions but with α_c=1 and then for pure AS and α_c=1. The delay observed for the anthropogenic cases modelled with α_c of 0.044 leads to an N_d that is 1.13–1.53 times higher than the case with the same chemical compositions but with α_c=1 (Table 2). This lower α_c also results in an N_d that is identical (for the 20 cm s^{-1} simulation) and 1.22 times higher (for the 100 cm s^{-1} simulation) compared to that for pure AS (α_c=1). If we assume α_c increases with the accumulation of water on the particles, the N_d decreases compared to the constant α_c simulations in the 100 cm s^{-1} simulation. In this case, the larger particles activate readily, increasing their α_c and depleting the excess water vapour so that the smaller sizes, for which the α_c remains lower, are unable to activate. Thus, depending on if and how α_c changes during the condensation process, the anthropogenic organic components may either enhance or diminish the indirect effect. Overall, these simulations suggest that the delay in the anthropogenic aerosol water uptake and the biogenic aerosol's lower κ_{org} compared to κ_{AS} may lead to slightly lower N_d than pure AS. The exception to this is if the α_c remains low throughout the droplet growth process; a possibility that seems unlikely.

A second effect that shows up in the modelling is of some significance to the indirect effect. Hypothetically, if the updraft velocity is the same but one case has a reduced growth rate compared to the other that leads to reduced N_d, then the adiabatic cloud LWC has to be reduced. Even if the N_d increase, persistently low growth rates (i.e. α_c=0.044) reduce the LWC in the case of the higher updraft speed (Table 2). At the lower updraft speed, the reduction in LWC for the variable α_c is about 0.03%, whereas the reduction for the higher updraft is about 0.4% compared to pure AS. This indicates that at least at cloud base and for higher updraft speeds, there can be insufficient time for the droplets to reach equilibrium when organic components from anthropogenic sources are present in the aerosol.

With a persistent smaller α_c, the N_d are higher because the cloud base supersatu-

ACPD
9, 13775–13799, 2009

ration is increased. However, the effect of the higher N_d may be offset by a reduction in LWC. In the more likely situation where the α_c starts relatively low and increases as the droplets increase in size, the effects of anthropogenic organics on the growth rates is to reduce both the cloud N_d and LWC. This result should not suggest that anthropogenic organics in general overall reduce the indirect effect of aerosol particles because the organic aerosol also influences the number concentrations of CCN and may enhance the indirect effect through that process (Leaitch et al., 2009). It is important to understand all of the ways that the organic aerosol can influence clouds.

4 Conclusions

For a study with both air of biogenic and anthropogenic influence, kinetics of the initial growth of cloud droplets in a CCN counter were measured and simulated. The organic components in the anthropogenic aerosol delayed the initial growth of these particles into cloud droplets when compared with a pure ammonium sulphate (AS) aerosol (S=0.35%, 0.1 μm particles). The best agreement between the observations and simulations was found for κ_{org}=0 and an average mass accommodation coefficient of α_c=0.044. A different effect was observed for fresher biogenic particles, where the organic-dominated particles exhibited similar initial growth rates as pure AS particles. The best agreement between the observations and simulations in these cases was found for κ_{org}=0.05–0.2 and α_c=1. Higher values of κ_{org} are possible but that requires decreased α_c in order to match the modelled and observed growth rates. The delay in the initial growth of the cloud droplets on anthropogenic aerosols suggest organic inhibition, possibly due to the formation of an organic film that coated the aerosol. Even though the biogenic aerosol appears to be fresher, it takes up water readily perhaps because the fresh secondary organic compounds from the oxidation of forest emissions are soluble. Ruehl et al. (2008) observed droplet growth inhibition (normalized to lab-generated AS) for aerosols in urban, polluted and continental air masses, consistent with the findings from our study.

ACPD
9, 13775–13799, 2009

Applying these findings in an adiabatic cloud parcel model, we find that the delay in the anthropogenic aerosol water uptake could increase (constant low α_c) or decrease (increasing α_c with increasing liquid water on the droplets) the N_d compared to either an aerosol with the same chemical composition and α_c=1 or a pure AS aerosol also with α_c=1. If α_c starts at a lower value and increases as more water accumulates on the droplet, the model results show a lower N_d and LWC, which slightly reduces the indirect effect. The biogenic aerosol's κ_{org} also appears to lead to slightly lower N_d compared with the pure AS simulation.

Acknowledgements. Thank-you to F. Froude and H. Dryfhout-Clark for meteorological information and to C. Green and the staff at the Centre for Atmospheric Research Experiments of Environment Canada for use of the facility and help during the study. Thanks to A. Gaudenzi, D. Halpin, S. Sharma, S. Sjostedt, D. Toom-Sauntry and A. Vlasenko throughout the field campaign and to L. M. Russell for helpful discussions. The authors gratefully acknowledge the NOAA Air Resources Laboratory for the provision of the HYSPLIT transport and dispersion model website (http://www.arl.noaa.gov/ready.html) used in this publication. The authors thank CFCAS for financial support, through the Cloud-Aerosol Feedbacks and Climate Network. Support to SOCAAR for the AMS came from CFI and OIT. R. Y.-W. Chang was supported by an NSERC CGS-D Scholarship.

References

Abbatt, J. P. D., Broekhuizen, K., and Kumar, P. P.: Cloud condensation nucleus activity of internally mixed ammonium sulfate/organic acid aerosol particles, Atmos. Environ., 39, 4767–4778, 2005.

Broekhuizen, K., Chang, R. Y. W., Leaitch, W. R., Li, S. M., and Abbatt, J. P. D.: Closure between measured and modeled cloud condensation nuclei (CCN) using size-resolved aerosol compositions in downtown Toronto, Atmos. Chem. Phys., 6, 2513–2524, 2006, http://www.atmos-chem-phys.net/6/2513/2006/.

Canagaratna, M. R., Jayne, J. T., Jimenez, J. L., Allan, J. D., Alfarra, M. R., Zhang, Q., Onasch, T. B., Drewnick, F., Coe, H., Middlebrook, A., Delia, A., Williams, L. R., Trimborn, A. M.,

Northway, M. J., DeCarlo, P. F., Kolb, C. E., Davidovits, P., and Worsnop, D. R.: Chemical and microphysical characterization of ambient aerosols with the aerodyne aerosol mass spectrometer, Mass Spectrom. Rev., 26, 185–222, 2007.

Chan, T. W., Huang, L., Leaitch, W. R., Sharma, S., Brook, J. R., Slowik, J. G., Abbatt, J. P. D., Brickell, P. C., Liggio, J., Li, S.-M., and Moosmüller, H.: Determination of OM/OC ratios and specific attenuation coefficients in ambient fine PM at a rural site in southern Ontario: Implications for emission sources, particle aging, and radiative forcing, Atmos. Chem. Phys. Discuss., in review, 2009.

Chang, R. Y. W., Liu, P. S. K., Leaitch, W. R., and Abbatt, J. P. D.: Comparison between measured and predicted CCN concentrations at Egbert, Ontario: Focus on the organic aerosol fraction at a semi-rural site, Atmos. Environ., 41, 8172–8182, 2007.

Chuang, P. Y., Charlson, R. J., and Seinfeld, J. H.: Kinetic limitations on droplet formation in clouds, Nature, 390, 594–596, 1997.

Chuang, P. Y.: Measurement of the timescale of hygroscopic growth for atmospheric aerosols, J. Geophys. Res.-Atmos., 108, 4282, doi:10.1029/2002JD002757, 2003.

Cruz, C. N., and Pandis, S. N.: A study of the ability of pure secondary organic aerosol to act as cloud condensation nuclei, Atmos. Environ., 31, 2205–2214, 1997.

Davidovits, P., Worsnop, D. R., Jayne, J. T., Kolb, C. E., Winkler, P., Vrtala, A., Wagner, P. E., Kulmala, M., Lehtinen, K. E. J., Vesala, T., and Mozurkewich, M.: Mass accommodation coefficient of water vapor on liquid water, Geophys. Res. Lett., 31, L22111, doi:10.1029/2004GL020835, 2004.

Drewnick, F., Hings, S. S., DeCarlo, P., Jayne, J. T., Gonin, M., Fuhrer, K., Weimer, S., Jimenez, J. L., Demerjian, K. L., Borrmann, S., and Worsnop, D. R.: A new time-of-flight aerosol mass spectrometer (TOF-AMS) – Instrument description and first field deployment, Aerosol Sci. Technol., 39, 637–658, 2005.

Duplissy, J., Gysel, M., Alfarra, M. R., Dommen, J., Metzger, A., Prevot, A. S. H., Weingartner, E., Laaksonen, A., Raatikainen, T., Good, N., Turner, S. F., McFiggans, G., and Baltensperger, U.: Cloud forming potential of secondary organic aerosol under near atmospheric conditions, Geophys. Res. Lett., 35, L03818, doi:10.1029/2007GL031075, 2008.

Engelhart, G. J., Asa-Awuku, A., Nenes, A., and Pandis, S. N.: CCN activity and droplet growth kinetics of fresh and aged monoterpene secondary organic aerosol, Atmos. Chem. Phys., 8, 3937–3949, 2008, http://www.atmos-chem-phys.net/8/3937/2008/.

Hartz, K. E. H., Rosenorn, T., Ferchak, S. R., Raymond, T. M., Bilde, M., Donahue, N. M., and Pandis, S. N.: Cloud condensation nuclei activation of monoterpene and sesquiterpene secondary organic aerosol, J. Geophys. Res.-Atmos., 110, 1–8, 2005.

Jayne, J. T., Leard, D. C., Zhang, X. F., Davidovits, P., Smith, K. A., Kolb, C. E., and Worsnop, D. R.: Development of an aerosol mass spectrometer for size and composition analysis of submicron particles, Aerosol Sci. Technol., 33, 49–70, 2000.

Jimenez, J. L., Jayne, J. T., Shi, Q., Kolb, C. E., Worsnop, D. R., Yourshaw, I., Seinfeld, J. H., Flagan, R. C., Zhang, X. F., Smith, K. A., Morris, J. W., and Davidovits, P.: Ambient aerosol sampling using the Aerodyne Aerosol Mass Spectrometer, J. Geophys. Res.-Atmos., 108, 8425, doi:10.1029/2001JD001213, 2003.

Kanakidou, M., Seinfeld, J. H., Pandis, S. N., Barnes, I., Dentener, F. J., Facchini, M. C., Van Dingenen, R., Ervens, B., Nenes, A., Nielsen, C. J., Swietlicki, E., Putaud, J. P., Balkanski, Y., Fuzzi, S., Horth, J., Moortgat, G. K., Winterhalter, R., Myhre, C. E. L., Tsigaridis, K., Vignati, E., Stephanou, E. G., and Wilson, J.: Organic aerosol and global climate modelling: a review, Atmos. Chem. Phys., 5, 1053–1123, 2005, http://www.atmos-chem-phys.net/5/1053/2005/.

Laaksonen, A., Vesala, T., Kulmala, M., Winkler, P. M., and Wagner, P. E.: Commentary on cloud modelling and the mass accommodation coefficient of water, Atmos. Chem. Phys., 5, 461–464, 2005, http://www.atmos-chem-phys.net/5/461/2005/.

Leaitch, W. R., Bottenheim, J. W., Biesenthal, T. A., Li, S. M., Liu, P. S. K., Asalian, K., Dryfhout-Clark, H., Hopper, F., and Brechtel, F.: A case study of gas-to-particle conversion in an eastern Canadian forest, J. Geophys. Res.-Atmos., 104, 8095–8111, 1999.

Leaitch, W. R., Russell, L. M., Lohmann, U., Shantz, N. C., Garrett, T., Toom-Sauntry, D., Strapp, J. W., Hayden, K. L., Marshall, J., Worsnop, D., and Jayne, J.: Do carbonaceous particles produce brighter clouds than sulphate particles?, Nature Geosci., in review, 2009.

Liu, P. S. K., Deng, R., Smith, K. A., Williams, L. R., Jayne, J. T., Canagaratna, M. R., Moore, K., Onasch, T. B., Worsnop, D. R., and Deshler, T.: Transmission efficiency of an aerodynamic focusing lens system: Comparison of model calculations and laboratory measurements for the Aerodyne Aerosol Mass Spectrometer, Aerosol Sci. Technol., 41, 721–733, 2007.

Marek, R. and Straub, J.: Analysis of the evaporation coefficient and the condensation coefficient of water, Int. J. Heat Mass Transf., 44, 39–53, 2001.

Medina, J., Nenes, A., Sotiropoulou, R. E. P., Cottrell, L. D., Ziemba, L. D., Beckman, P. J.,

and Griffin, R. J.: Cloud condensation nuclei closure during the International Consortium for Atmospheric Research on Transport and Transformation 2004 campaign: Effects of size-resolved composition, J. Geophys. Res.-Atmos., 112, D10S31, doi:10.1029/2006JD007588, 2007.

Ming, Y. and Russell, L. M.: Organic aerosol effects on fog droplet spectra, J. Geophys. Res.-Atmos., 109, 13–14, 2004.

Mozurkewich, M.: Aerosol Growth and the Condensation Coefficient for Water – a Review, Aerosol Sci. Technol., 5, 223–236, 1986.

Petters, M. D. and Kreidenweis, S. M.: A single parameter representation of hygroscopic growth and cloud condensation nucleus activity, Atmos. Chem. Phys., 7, 1961–1971, 2007, http://www.atmos-chem-phys.net/7/1961/2007/.

Prenni, A. J., Petters, M. D., Kreidenweis, S. M., DeMott, P. J., and Ziemann, P. J.: Cloud droplet activation of secondary organic aerosol, J. Geophys. Res., 112, D10223, doi:10.1029/2006JD007963, 2007.

Ruehl, C. R., Chuang, P. Y., and Nenes, A.: How quickly do cloud droplets form on atmospheric particles?, Atmos. Chem. Phys., 8, 1043–1055, 2008, http://www.atmos-chem-phys.net/8/1043/2008/.

Rupakheti, M., Lohmann, U., Leaitch, W. R., Hayden, K., Brickell, P., Lu, G., Li, S.-M., Toom-Sauntry, D., Bottenheim, J. W., Brook, J. R., Vet, R., Jayne, J. T., and Worsnop, D. R.: An intensive study of the size and composition of submicron atmospheric aerosols at a rural site in Ontario, Canada, Aerosol Sci. Technol., 39, 722–736, 2005.

Shantz, N. C., Leaitch, W. R., and Caffrey, P. F.: Effect of organics of low solubility on the growth rate of cloud droplets, J. Geophys. Res.-Atmos., 108, 4168–4176, 2003.

Shantz, N. C., Leaitch, W. R., Phinney, L., Mozurkewich, M., and Toom-Sauntry, D.: The effect of organic compounds on the growth rate of cloud droplets in marine and forest settings, Atmos. Chem. Phys., 8, 5869–5887, 2008, http://www.atmos-chem-phys.net/8/5869/2008/.

Shulman, M. L., Jacobson, M. C., Charlson, R. J., Synovec, R. E., and Young, T. E.: Dissolution behavior and surface tension effects of organic compounds in nucleating cloud droplets, Geophys. Res. Lett., 23, 277–280, 1996.

Slowik, J. G., Stroud, C., Bottenheim, J. W., Brickell, P. C., Chang, R. Y.-W., Liggio, J., Makar, P. A., Martin, R., Moran, M. D., Shantz, N. C., Sjostedt, S. J., van Donkelaar, A., Vlasenko, A., Wiebe, H. A., Xia, A. G., Zhang, J., Leaitch, W. R., and Abbatt, J. P. D.: A large biogenic

organic aerosol source from Eastern Canadian forests, Nature Geosci., submitted, 2009.
Stroud, C. A., Nenes, A., Jimenez, J. L., DeCarlo, P. F., Huffman, J. A., Bruintjes, R., Nemitz, E., Delia, A. E., Toohey, D. W., Guenther, A. B., and Nandi, S.: Cloud activating properties of aerosol observed during CELTIC, J. Atmos. Sci., 64, 441–459, 2007.
VanReken, T. M., Ng, N. L., Flagan, R. C., and Seinfeld, J. H.: Cloud condensation nucleus activation properties of biogenic secondary organic aerosol, J. Geophys. Res.-Atmos., 110, D07206, doi:10.1029/2004JD005465, 2005.
Vlasenko A., Slowik, J. G., Bottenheim, J. W., Brickell, P. C., Chang, R. Y.-W., Macdonald, A. M., Shantz, N. C., Sjostedt, S. J., Wiebe, H. A., Leaitch, W. R., and Abbatt, J. P. D.: PTR-MS VOC measurements at a rural Ontario site: sources and correlations to aerosol composition, J. Geophys. Res., in review, 2009.
Zhang, Q., Jimenez, J. L., Canagaratna, M. R., Allan, J. D., Coe, H., Ulbrich, I., Alfarra, M. R., Takami, A., Middlebrook, A. M., Sun, Y. L., Dzepina, K., Dunlea, E., Docherty, K., DeCarlo, P. F., Salcedo, D., Onasch, T., Jayne, J. T., Miyoshi, T., Shimono, A., Hatakeyama, S., Takegawa, N., Kondo, Y., Schneider, J., Drewnick, F., Borrmann, S., Weimer, S., Demerjian, K., Williams, P., Bower, K., Bahreini, R., Cottrell, L., Griffin, R. J., Rautiainen, J., Sun, J. Y., Zhang, Y. M., and Worsnop, D. R.: Ubiquity and dominance of oxygenated species in organic aerosols in anthropogenically-influenced Northern Hemisphere midlatitudes, Geophys. Res. Lett., 34, L13801, doi:10.1029/2007GL029979, 2007.

Table 1. Observations from the size-selected nearly monodisperse ambient aerosol of stronger anthropogenic influence. Simulations were used to determine α_c for the anthropogenic cases compared to AS calibration simulations (assuming α_c of unity). The organics in the simulations are assumed to have κ_{org} of zero.

Date (dd mmm)	Time	D_{geo} (μm)	Number conc. (cm^{-3})	Organic mass fraction at D_{geo}	Inorganic mass fraction at D^a_{geo}	Approx. delay time (sec)	α_c estimated range	α_c midpoint of estimated range
27 May	13:33–14:05	0.12	95–105	0.53	0.47	1	0.03–0.05	0.04
7 Jun	16:37–16:42	0.10	285–295	0.40	0.60	1	0.04–0.07	0.055
7 Jun	16:44–16:58	0.10	265-275	0.40	0.60	1.25	0.03–0.05	0.04
7 Jun	17:01–18:00	0.10	215–225	0.38	0.62	1	0.04–0.06	0.05
7 Jun	18:00–18:17	0.10	205–215	0.39	0.61	0.75	0.05–0.07	0.06
8 Jun	11:26–11:46	0.10	65–75	0.48	0.52	1	0.01–0.03	0.02
						Average α_c		0.044
						Standard deviation of α_c		0.014

[a] Inorganic is assumed to be ammonium sulphate with κ_{AS} of 0.61.

ACPD
9, 13775–13799, 2009

Table 2. Simulations from the adiabatic cloud parcel model for anthropogenic and biogenic case studies. The total mass fractions, hygroscopicity parameters (κ) and mass accommodation coefficients (α_c) are unitless. The number of droplets (N_d) found in these simulated clouds is determined well above the maximum supersaturation (60 m above cloud base) for 2 updraft velocities (u), 20 and 100 cm s^{-1}. "Anth" is anthropogenic aerosol, "Biog" is biogenic aerosol and "AS" indicates a simulation that modelled the ambient size distribution from the date indicated but with the composition as pure ammonium sulphate. All simulations are scaled to the same total number concentration of 1500 cm^{-3}. Also, only particles >0.05 μm are simulated here.

		Total Mass Fraction					u=20 cm s^{-1}	u=100 cm s^{-1}	u=20 cm s^{-1}	u=100 cm s^{-1}
Date (dd mmm)	Case	Org.	Inorg.[a]	κ_{org}	κ_{AS}	α_c	LWC (g m^{-3})	LWC (g m^{-3})	N_d (cm^{-3})	N_d (cm^{-3})
7 Jun	Anth	0.37	0.63	0	0.61	0.044	0.12816	0.13513	269	936
7 Jun	Anth	0.37	0.63	0	0.61	Vary 0.01 to 1[b]	0.13068	0.13535	238	565
7 Jun	Anth	0.37	0.63	0	0.61	1	0.13082	0.13535	238	612
7 Jun	AS	0	1	N/A	0.61	1	0.13115	0.13539	269	768
11 Jun	Biog	0.78	0.22	0.2	0.61	1	0.13135	0.13544	292	885
11 Jun	AS	0	1	N/A	0.61	1	0.13148	0.13992	364	995

[a] Inorganic is assumed to be ammonium sulphate.

[b] α_c is assumed to increase as the amount of liquid water on the droplets increase.

ACPD
9, 13775–13799, 2009

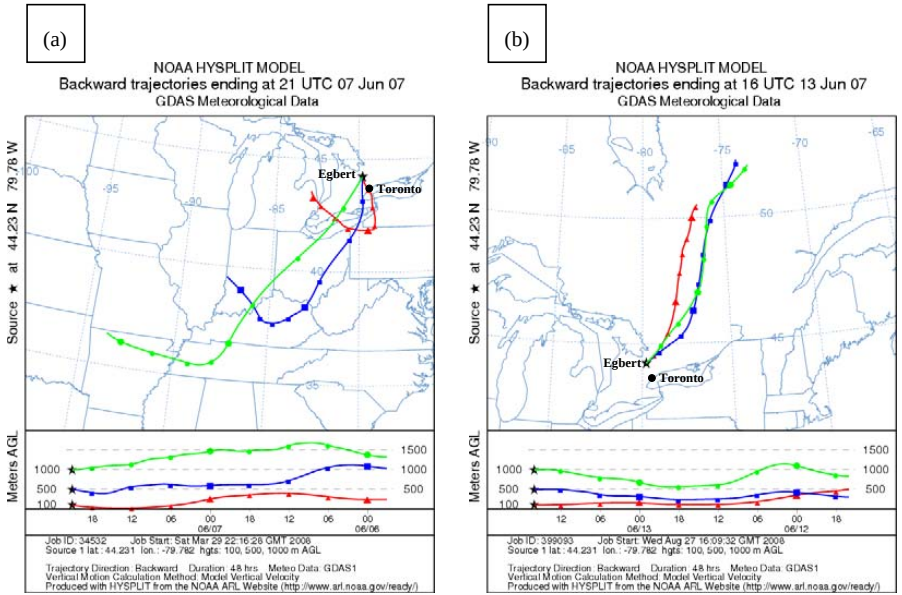

Fig. 1. Back trajectory analyses from the NOAA Air Resources Laboratory HYSPLIT program for **(a)** an anthropogenically influenced period (7 June) and **(b)** a biogenically influenced period (13 June). Egbert, Ontario is the trajectory end point.

ACPD
9, 13775–13799, 2009

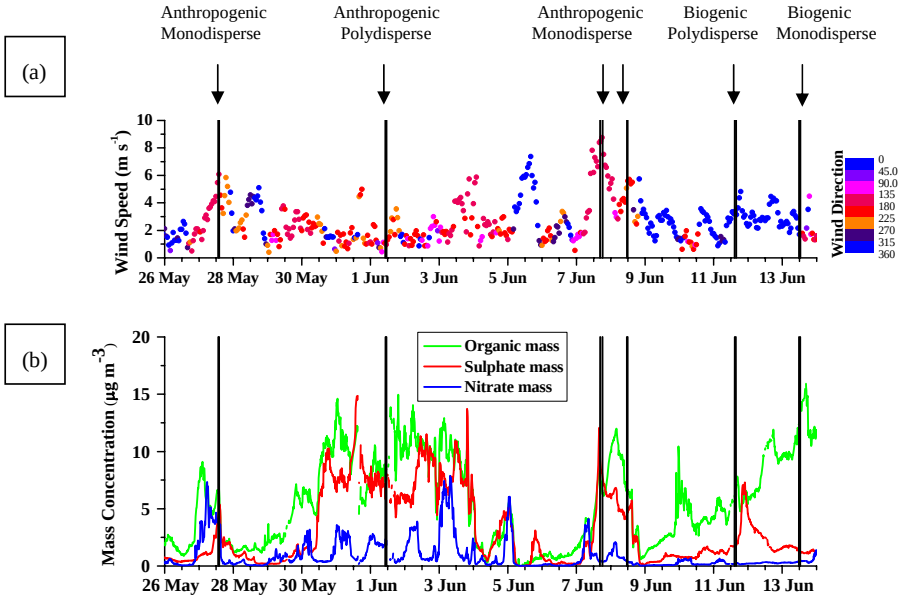

Fig. 2. Time Series from Egbert 2007 of **(a)** wind speed, colour-coded to wind direction (reds=south winds, blues=north winds) and **(b)** organic, sulphate and nitrate data from the C-ToF AMS. Indicated in black lines are the case study periods discussed in this paper. Dates/times are in EDT, local time (LT).

ACPD
9, 13775–13799, 2009

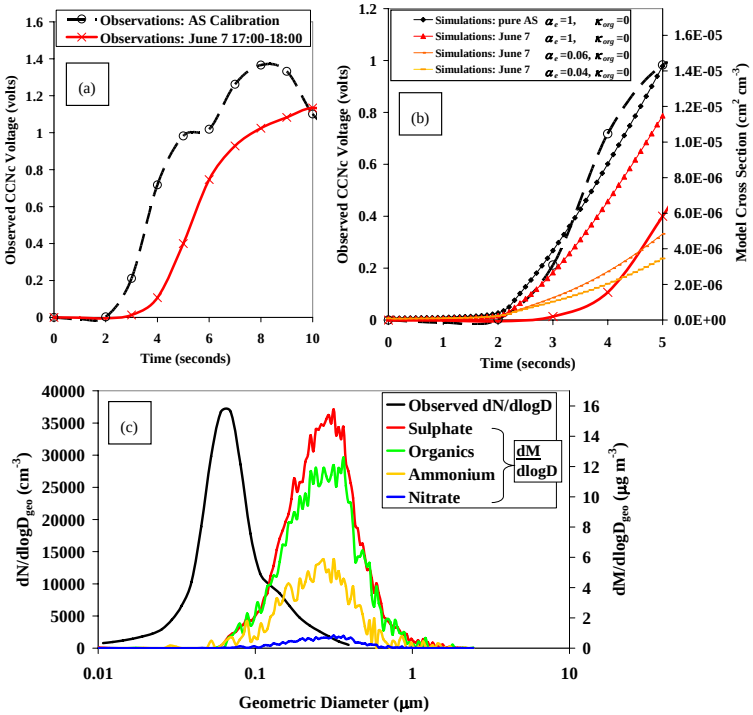

Fig. 3. 7 June 2007, 17:00–18:00 LT anthropogenic case with south winds. **(a)** Observations of CCN counter droplet growth rates (shown as a voltage) size-selected to 0.1 μm at S=0.35% and number concentrations of 215–225 cm^{-3}. The x-axis is the sample time as the particles activate and grow into cloud droplets. **(b)** The observed growth rates from the CCN counter from (a) correspond to the left y-axis. The right y-axis show the droplet cross-sectional area calculated in the simulations. The simulations assume 62% AS (κ_{AS}=0.61) and 38% organic mass fractions (κ_{org}=0) for a nearly monodisperse aerosol centred around 0.1 μm. This figure is constrained to 5 s because the model does not simulate the droplet gravitational settling. **(c)** Mass distributions from the AMS particle time-of-flight measurements (right y-axis) and number size distributions (left y-axis) from the SMPS. The x-axis shows the geometric diameter (converted from D_{va} assuming a particle density of 1.63 g cm^{-3}, calculated as described in Sect. 3.2).

ACPD
9, 13775–13799, 2009

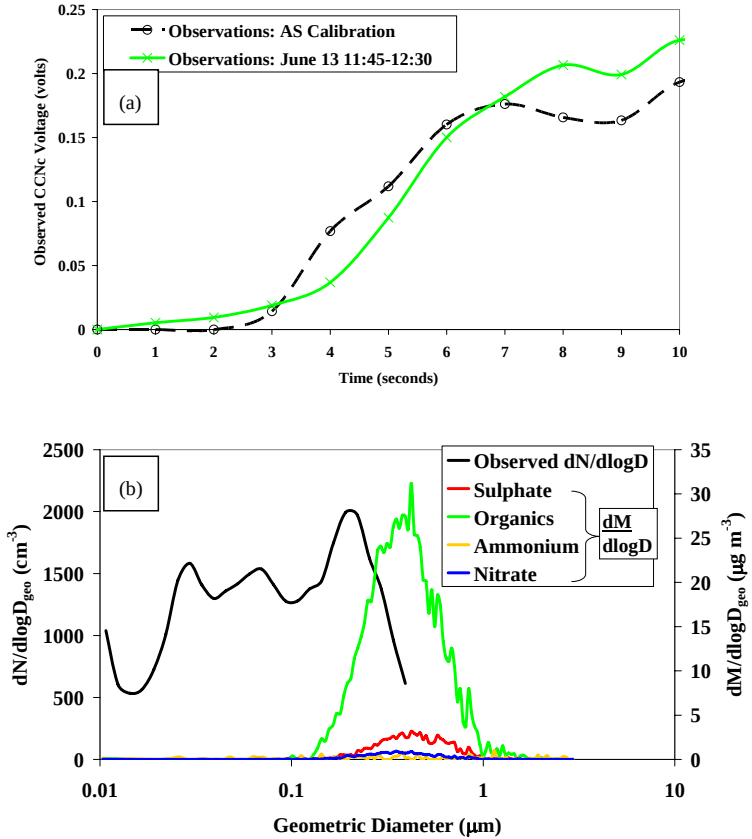

Fig. 4. 13 June 2007, 11:45–12:30 LT biogenic case with north winds. **(a)** Observations of CCN counter droplet growth rates size-selected to 0.12 μm at S=0.35% and number concentrations of 35–45 cm^{-3}. **(b)** Mass distributions (11:00–12:00) from the AMS particle time-of-flight measurements and number size distributions from the SMPS (11:45–12:30). The x-axis shows the geometric diameter (converted from D_{va} assuming a particle density of 1.38 g cm^{-3}).

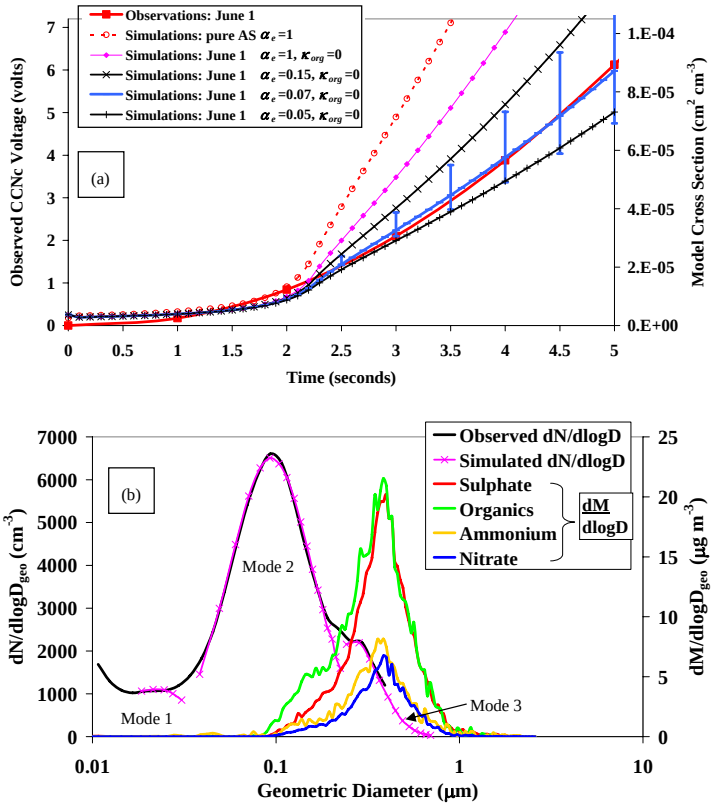

Fig. 5. 1 June 2007, 10:26–11:05 LT anthropogenic case with south winds. **(a)** Observations of CCN counter droplet growth rates for polydisperse ambient aerosol measured at S=0.35%. The red solid line is the observed growth rate from the CCN counter (left y-axis) and all other curves are modelled growth rates shown as cross-sectional area (right y-axis). The error bars demonstrate simulations performed at S=±0.05% to reflect the error in the calculated supersaturation. **(b)** Observed (black) and modelled (pink) number size distribution (left y-axis) and observed mass distributions from the AMS particle time-of-flight measurements (right y-axis). The D_{va} have been converted to geometric diameter assuming a particle density of 1.54 g cm^{-3}.

ACPD
9, 13775–13799, 2009

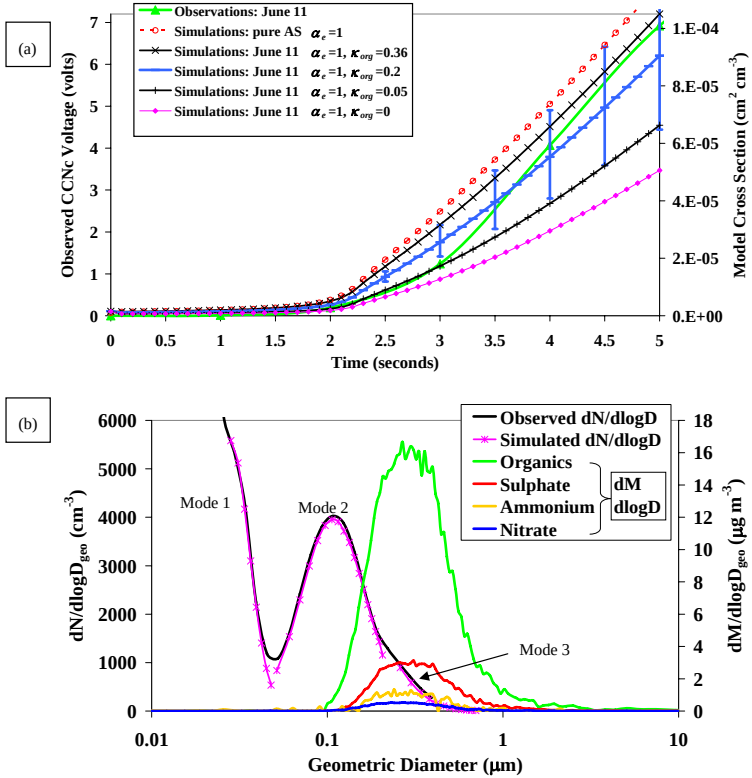

Fig. 6. 11 June 2007, 14:45–15:35 LT biogenic case with north winds. **(a)** Observations of CCN counter droplet growth rates for polydisperse ambient aerosol measured at S=0.35%. The green solid line is the observed growth rate from the CCN counter (left y-axis) and all other curves are modelled growth rates shown as cross-sectional area (right y-axis). **(b)** Observed (black) and modelled (pink) number size distribution (left y-axis) and mass distributions from the AMS particle time-of-flight measurements (right y-axis). The D_{va} have been converted to geometric diameter assuming a particle density of 1.4 g cm^{-3}.